



Amplification of the human epidermal growth factor receptor 2 (*HER2*) gene is associated with a microsatellite stable status in Chinese gastric cancer patients

He Huang^{1#}, Zhengkun Wang^{2#}, Yi Li², Qun Zhao³, Zhaojian Niu²

¹Department of Gastrointestinal Surgery, The First Hospital of Shanxi Medical University, Shanxi, China; ²Department of Gastrointestinal Surgery, The Affiliated Hospital of Qingdao University, Qingdao, China; ³Department of Gastrosurgery, The Fourth Hospital of Hebei Medical University, Shijiazhuang, China

Contributions: I) Conception and design: Z Niu, Q Zhao, H Huang; (II) Administrative support: Z Niu, H Huang, Z Wang; (III) Provision of study materials or patients: All authors; (IV) Collection and assembly of data: Z Wang, Q Zhao; (V) Data analysis and interpretation: Z Niu, H Huang; (VI) Manuscript writing: All authors; (VII) Final approval of manuscript: All authors.

[#]These authors contributed equally to this work.

Correspondence to: Zhaojian Niu. Department of Gastrointestinal Surgery, The Affiliated Hospital of Qingdao University, No. 16, Jiangsu Road, Shinan District, Qingdao 260003, China. Email: 18678922277@163.com; Qun Zhao. Department of Gastrosurgery, The Fourth Hospital of Hebei Medical University, No. 12 Jiankang Road, Shijiazhuang 050011, China. Email: zhaoqun516@126.com.

Background: Gastric cancer (GC) is one of the most common cancers worldwide. However, little is known about the combination of *HER2* amplification and microsatellite instability (MSI) status in GC. This study aimed to analyze the correlation of *HER2* amplification with microsatellite instability (MSI) status, clinical characteristics, and the tumor mutational burden (TMB) of patients.

Methods: A total of 192 gastric cancer (GC) patients were enrolled in this cohort. To analyze genomic alterations (GAs), deep sequencing was performed on 450 target cancer genes. TMB was measured by an in-house algorithm. MSI status was inferred based on the MANTIS (Microsatellite Analysis for Normal-Tumor InStability) score.

Results: The most frequently amplified genes in the GC patients included cyclin E1 (*CCNE1*), human epidermal growth factor receptor 2 (*HER2*), fibroblast growth factor receptor 2 (*FGFR2*), cyclin D1 (*CCND1*), fibroblast growth factor 19 (*FGF19*), fibroblast growth factor 3 (*FGF3*), and fibroblast growth factor 4 (*FGF4*). The frequency of *HER2* amplification was 9.38% (18/192). *HER2* amplification was higher in females than in males (14.52% *vs.* 6.92%, respectively, $P=0.091$), however, MSI was higher in males compared to females (7.69% *vs.* 4.84%, respectively, $P=0.46$). *HER2* amplification was higher in metastatic loci compared to primary lesions (23.08% *vs.* 8.38%, respectively, $P=0.079$) and was lower in patients with high TMB (TMB-H) compared to those with low TMB (TMB-L) (4.0% *vs.* 11.35%, respectively, $P=0.12$). While the frequency of MSI in metastatic foci was higher than that in primary lesions (15.38% *vs.* 6.15%, respectively, $P=0.48$), MSI status was highly associated with TMB-H (20% *vs.* 0%, respectively, $P=3.66\times 10^{-7}$). Furthermore, *HER2* amplification was negatively correlated with MSI status in Chinese GC patients.

Conclusions: *HER2* amplification was negatively correlated with TMB-H and MSI status, and MSI status was significantly associated with TMB-H in Chinese GC patients. These data suggested that *HER2* amplification might be a negative indicator for GC immunotherapy.

Keywords: Gastric cancer (GC); human epidermal growth factor receptor 2 amplification; microsatellite instability (MSI); tumor mutational burden (TMB); biomarker

Submitted Dec 10, 2020. Accepted for publication Apr 04, 2021.

doi: 10.21037/jgo-21-47

View this article at: <http://dx.doi.org/10.21037/jgo-21-47>

Introduction

Gastric cancer (GC) is one of the most common cancers worldwide, with the highest rates observed in Europe and Eastern Asia (1). Surgical resection is the primary treatment for GC with good efficacy in patients who are diagnosed early. However, the survival rate of late-stage cancer patients is still extremely low (2,3). To date, a series of next-generation sequencing (NGS) studies, including those from The Cancer Genome Atlas (TCGA), have revealed several genes that are frequently mutated in GC (4,5), facilitating the development of targeted gene therapy to effectively improve the overall survival of GC patients (6,7).

Human epidermal growth factor receptor 2 (*HER2*), also known as erb-b2 receptor tyrosine kinase 2 (*ERBB2*), is a human growth factor receptor that regulates cell growth and differentiation (8). High levels of *HER2* amplification can induce the overexpression of cell membrane proteins and subsequently, the cells acquire the characteristics of malignant cells (9). Trastuzumab is a drug that targets the *HER2* protein to improve the survival rate of patients with primary and metastatic *HER2*-positive breast cancer (10). Mutations of *HER2* often occur in a variety of cancers, such as breast cancer, lung cancer, and GC (11). The positive rate of *HER2* in GC increased with age and was positively correlated with the intestinal type (12). *HER2* protein expression also associated with tumor differentiation, Lauren classification, Borrmann type, and P53 expression in GC (13). Many reports have shown a poor prognosis for patients with *HER2*-positive tumors compared to those with *HER2*-negative tumors (14-16). Unlike breast cancer, the correlation between *HER2* and prognosis in GC patients remains controversial. Some studies have shown that *HER2*-positive tumors are associated with a significantly deteriorating prognosis, while others have shown that *HER2* status is not related to prognosis (16-20).

Microsatellite instability (MSI) is a description of genomic instability caused by the inactivation of DNA mismatch repair genes (21). MSI is considered to be a positive prognosis biomarker and high MSI (MSI-H) is associated with a good prognosis in many cancers, especially in colorectal cancer (CRC) (22,23). MSI has also been associated with good prognosis and low lymph node metastasis in GC patients (24,25).

The prognostic predictions of MSI and *HER2* amplification are different. *HER2* amplification is associated with a poor prognosis, while MSI is associated with a good prognosis. In patients with *HER2* positive gastric cancer,

the addition of trastuzumab in the first-line chemotherapy can improve the survival rate (26,27). *HER2* targeted therapy in gastric cancer was selected as the first-line treatment in *HER2* positive patients. MSI is also considered in adjuvant immunotherapy (27). However, little is known regarding the combination of these two indicators in GC. This study identified the mutational profiling of 192 GC cases and analyzed the relationship between *HER2* and MSI, and the relationship between *HER2* and TMB, and aimed to guide the selection and effectiveness of targeted therapy for gastric cancer patients.

We present the following article in accordance with the MDAR reporting checklist (available at <http://dx.doi.org/10.21037/jgo-21-47>).

Methods

Patient enrollment and sample collection

All procedures performed in this study involving human participants were in accordance with the Declaration of Helsinki (as revised in 2013). The study was approved by institutional ethics committee of The First Hospital of Shanxi Medical University (No.: 2020-K008) and informed consent was taken from all the patients. A total of 192 Chinese GC patients were randomly enrolled in this study. Both formalin-fixed and paraffin-embedded (FFPE) tumor tissues, and matched blood samples were collected from patients for the detection of genomic alterations (GAs) using the NGS-based YuanSuTM450 gene panel (Origimed, Shanghai, China). Genomic DNA was isolated using the QIAamp DNA FFPE Tissue Kit and the QIAamp DNA Blood Midi Kit (Qiagen, Hilden, Germany) according to the manufacturer's instructions. The concentration of DNA was measured by Qubit (Life Technologies) and normalized to 20–50 ng/μL.

Identification of GAs, TMB, and MSI

The genomic profile was produced using the YuanSuTM450 gene panel (Appendix 1), which covers all the coding exons of the 450 cancer-related genes, and 64 selected introns in the 39 genes that are frequently rearranged in solid tumors (28). The genes were captured and sequenced with a mean depth of 800× by using Illumina NextSeq 500 (Illumina, Inc., CA). Single nucleotide variants (SNVs) were identified by MuTect (v1.17). Insertion-deletion polymorphisms (indels) were identified by using PINDEL

Table 1 Clinicopathologic features of 192 Chinese GC patients

Variable	N=192
Gender	
Male	130
Female	62
Age (years), median (range)	62 (27–86)
TMB, median (range)	5.4 (0–83.7)
Lesion	
Primary	179
Metastases	13
Differentiated degree	
Well/moderately differentiated	30
Poorly/undifferentiated	129
Not available	33

GC, gastric cancer; TMB, tumor mutational burden.

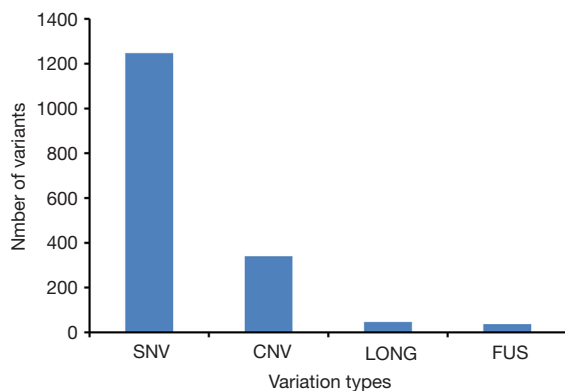


Figure 1 Statistical distribution map of variation types. SNV, single nucleotide variant; CNV, copy number variation; LONG, long insertion/deletion; FUS, gene fusion.

(V0.2.4). The functional impact of these mutations was annotated by SnpEff3.0. Copy number variation (CNV) regions were identified by Control-FREEC (v9.4) with the following parameters: window =50,000, and step =10,000. Gene fusions were detected through an in-house pipeline. Gene rearrangements were assessed by Integrative Genomics Viewer (IGV). TMB is a measure of the number of somatic mutations per megabase of genome coding region. With the reference to previous method (29), TMB was estimated by counting the somatic mutations in coding area, including SNVs and indels, per megabase of

the sequence examined. MSI status was inferred based on the MANTIS (Microsatellite Analysis for Normal Tumor InStability) score (30), and microsatellite regions were manually reviewed using the Integrated Genomics Viewer (IGV) for confirmation.

Statistical analysis

Statistical analyses were performed using SPSS version 22.0 (SPSS Inc., Chicago, IL, USA). Fisher's exact test was used to analyze significant differences. $P < 0.05$ was considered statistically significant.

Results

Characteristics of Chinese GC patients

In this cohort, a total of 192 Chinese GC patients, including 130 (67.71%) males and 62 (32.29%) females, were enrolled. The median age was 62 years old (range, 27–86 years old). Samples from 179 (93.23%) original primary tumors and 13 (6.77%) metastatic tumors were collected. The degree of tumor differentiation was identified for 159 samples. There were 30 well or moderately differentiated samples and 129 poorly differentiated or undifferentiated samples (Table 1).

The mutational landscape and the frequency of high MSI (MSI-H) and HER2 amplification in Chinese GC patients

According to the sequencing results of the tumor samples, 1,670 clinically relevant GAs were identified in 361 genes, with a mean of 8.70 GAs per sample (range, 1–59) (Table S1). Among these alterations, 74.67% (1,247/1,670) were SNV/short indels, 20.36% (340/1,670) were CNVs, 2.22% (37/1,670) were fusion, and 2.75% (46/1,670) were long indel variations (Figure 1). The most frequently mutated genes with mutation frequencies greater than 10% included tumor protein P53 (*TP53*; 68.23%, 131/192), AT-rich interactive domain-containing protein 1A (*ARID1A*; 18.75%, 36/192), low-density lipoprotein receptor-related protein 1B (*LRP1B*; 17.19%, 33/192), *ERBB2* (14.58%, 28/192), protocadherin fat 4 (*FAT4*; 13.54%, 26/192), cadherin 1 (*CDH1*; 12.50%, 24/192), and cyclin E1 (*CCNE1*; 10.94%, 21/192) (Figure 2). The most frequently amplified genes included *CCNE1*, *HER2*, fibroblast growth factor receptor 2 (*FGFR2*), cyclin D1 (*CCND1*), fibroblast growth factor 19 (*FGF19*), fibroblast growth factor 3 (*FGF3*),

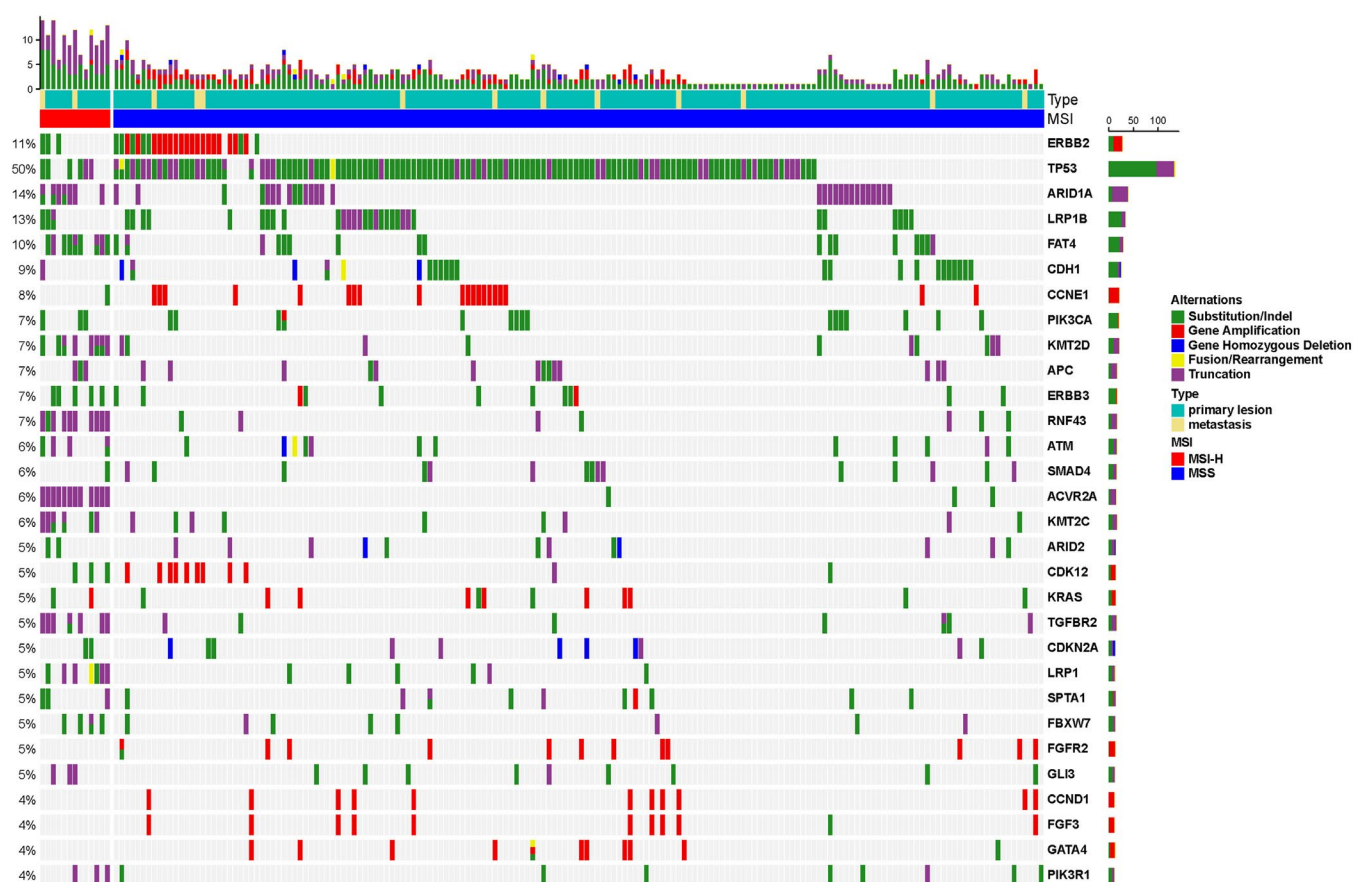


Figure 2 Mutational profiling of 192 Chinese gastric cancer patients. The X-axis represents each case sample and the Y-axis represents each mutated gene. The bar graph above shows the gene mutations of each sample, and the bar graph on the right shows the mutation frequency of each mutated gene in this cohort. In between the upper and lower panel, primary tumors are shown in light green, metastatic lesions are depicted in yellow, microsatellite stable (MSS) status is shown in blue, and the high level of microsatellite instability (MSI-H) is shown in red. The lower panel shows the genetic alterations for each sample. Green represents substitution/indel mutations, red represents gene amplification mutations, blue represents gene homozygous deletion mutations, yellow represents fusion/rearrangement mutations, and purple represents truncation mutations.

fibroblast growth factor 4 (*FGF4*), GATA binding protein 4 (*GATA4*), retinoic acid receptor alpha (*RARA*), and DNA topoisomerase 2-alpha (*TOP2A*). For *HER2*, there were 18 gene amplification mutations and 10 CNVs. The frequency of *HER2* amplification was 9.38% (18/192) (Table S1).

MSI-H and TMB are important biomarkers and were investigated in this cohort. According to previous studies, TMB values less than 10 were classified as low TMB (TMB-L) and TMB values greater than 10 were classified as high TMB (TMB-H) (31,32). Among the 192 GC patients in this study, 141 showed TMB-L, 50 showed TMB-H, and 1 patient did not have an available TMB value. The median TMB of this cohort was 5.4 Muts/Mb (range,

0–83.7). In addition, MSI was detected in 13 cases (13/192, 6.77%; Table 1). Together with the incidence rate of *HER2* amplification, these results were consistent with previously reported incidence rates (33–36).

The association between HER2 amplification, MSI, TMB value, tumor origin, gender, and age of patients

There were 18 *HER2*-positive cases, including 9 males and 9 females, aged from 37 to 75 years old. Based on statistical analysis, the detection of *HER2* amplification in females was higher than in males, but the difference was not statistically significant (14.52% vs. 6.92%, respectively, $P=0.091$;

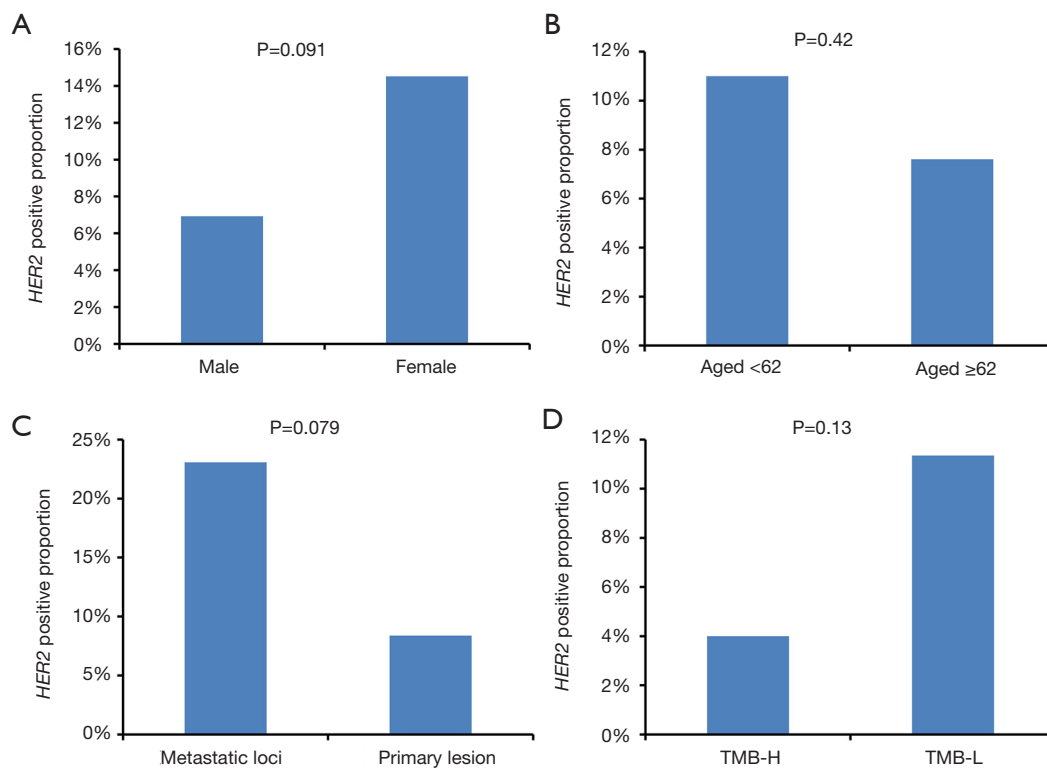


Figure 3 Correlation analysis of *HER2* amplification status and clinical features. (A) The correlation between *HER2* amplification status and gender; (B) the correlation between *HER2* amplification status and age of the patients; (C) the correlation between *HER2* amplification status and tumor origin; (D) the correlation between *HER2* amplification status and tumor mutational burden (TMB) value. *HER2*, human epidermal growth factor receptor 2.

Figure 3A). Based on the median age, patients were divided into two groups, those aged less than 62 years and those aged 62 years and older. In the *HER2* amplification positive cases, there were 7 patients aged less than 62 years, and 11 patients aged 62 years and older. There were no differences in *HER2* amplification between the two age groups (Figure 3B).

With the exception of 3 patients who presented with metastases, all tumors were primary lesions. TMB-H was found in 2 *HER2*-positive cases and TMB-L was found in the remaining 16 cases. The detection rate of *HER2* amplification in metastatic foci was higher than that in primary lesions (23.08% vs. 8.38%, respectively, $P=0.079$), and the frequency of *HER2* amplification in patients with TMB-H was lower than in patients with TMB-L (4.0% vs. 11.35%, respectively, $P=0.13$). However, the association between tumor sites and TMB was not statistically significant (Figure 3C,D).

In the 13 patients with MSI, including 10 males and 3 females, aged 43 to 82 years old, the frequency of MSI

detection was higher in males than in females, but the difference was not statistically significant (7.69% vs. 4.84%, respectively, $P=0.46$; Figure 4A). Similarly, MSI status in the different age groups was investigated. MSI status was detected in 5 patients aged less than 62 years, and 8 patients aged 62 years and older. No significant differences were detected in the MSI status between the two age groups (Figure 4B). The frequency of MSI in metastatic foci was higher than that in primary lesions (15.38% vs. 6.15%, respectively, $P=0.20$), however this was not statistically significant (Figure 4C). Interestingly, except for 1 patient with an unavailable TMB value, all 12 patients with MSI status also harbored TMB-H. Statistical analysis revealed that MSI status was highly associated with TMB-H (20% vs. 0%, respectively, $P=3.66 \times 10^{-7}$; Figure 4D).

HER2 amplification is negatively correlated with microsatellite status in Chinese gastric patients

A total of 18 *HER2* positive and 13 MSI cases were found

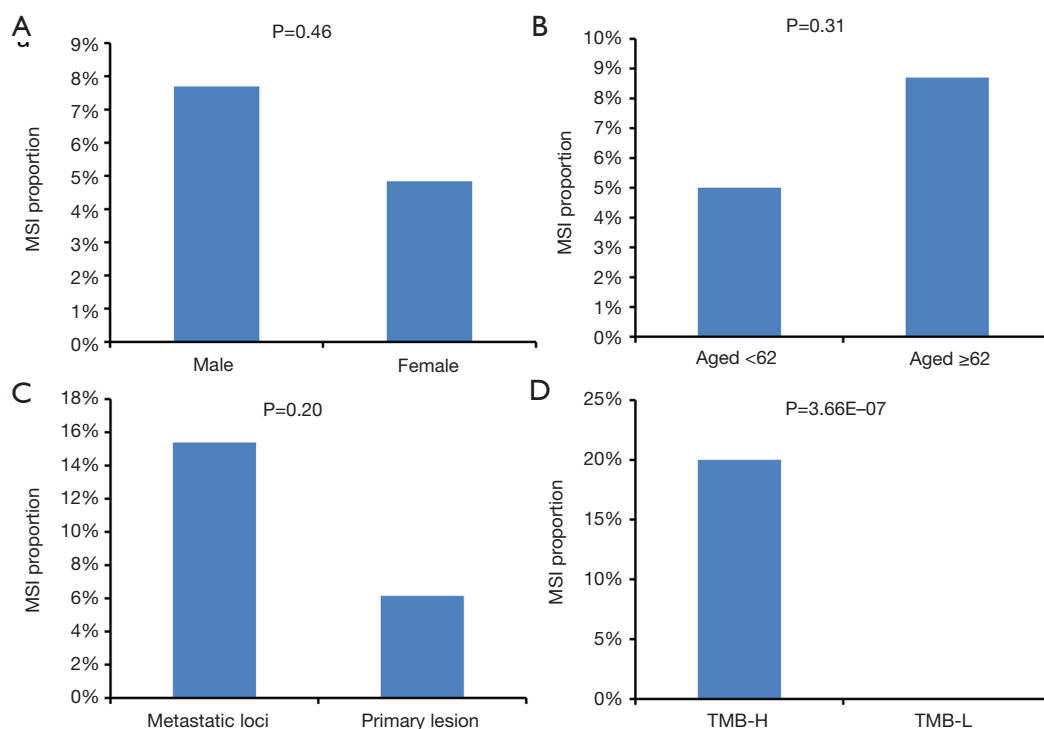


Figure 4 Correlation analysis of microsatellite instability (MSI) status and clinical features. (A) The correlation between MSI status and gender; (B) the correlation between MSI status and age of patients; (C) the correlation between MSI status and tumor origin; (D) the correlation between MSI status and tumor mutational burden (TMB) value.

in this study. However, none of the patients were detected as *HER2* positive and MSI positive concurrently. Statistical analysis demonstrated that there was no significant correlation between *HER2* positive and MSI (0% vs. 7.47%, respectively, $P=0.48$).

Interestingly, the proportion of *HER2* positive samples was higher in females than in males, while the proportion of MSI positive samples was lower in females than in males (Figures 3A,4A). Unexpectedly, no significant differences were detected between *HER2* and MSI in female patients (14.52% vs. 4.84%, respectively, $P=0.13$; Figure 5A).

Due to the significant correlation between MSI and TMB-H, we examined the correlation between *HER2* and MSI and TMB-H. As expected, the frequency of *HER2* positive cases was significantly lower than the frequency of MSI in TMB-H patients (4.0% vs. 20.0%, respectively, $P=0.031$) (Figure 5B).

Combining the occurrence of *HER2* positive and MSI and their correlation with the patient's gender and TMB value, we concluded that *HER2* amplification is negatively correlated with MSI in Chinese GC patients.

Discussion

GC is characterized by a high degree of biological heterogeneity, suggesting that each GC patient has varied genetic and molecular characteristics. With the development of NGS sequencing technology in the past decade, many studies have been focused on the mutational profiling of GC (5,37-40). In Caucasian patients, mutations were most commonly detected in the following genes: *TP53*, Kirsten rat sarcoma viral oncogene homolog (*KRAS*), *ARID1A*, phosphatidylinositol-4,5-bisphosphate 3-kinase catalytic subunit alpha (*PIK3CA*), *ERBB3*, phosphatase and tensin homolog (*PTEN*), and major histocompatibility complex, class I, B (*HLA-B*) (5). While in Korean GC patients, mutations were most commonly detected in the following genes: *TP53*, epidermal growth factor receptor (*EGFR*), hepatocyte nuclear factor 1-alpha (*HNF1A*), *PIK3CA*, and *ERBB2* (38). Jia *et al.* showed that the frequency of mutation in the adenomatous polyposis coli (*APC*), *ARID1A*, lysine methyltransferase 2A (*KMT2A*), *PIK3CA*, and *PTEN* genes were significantly different between Asian and Caucasian GC patients (39). For Chinese GC patients, Wang *et al.*

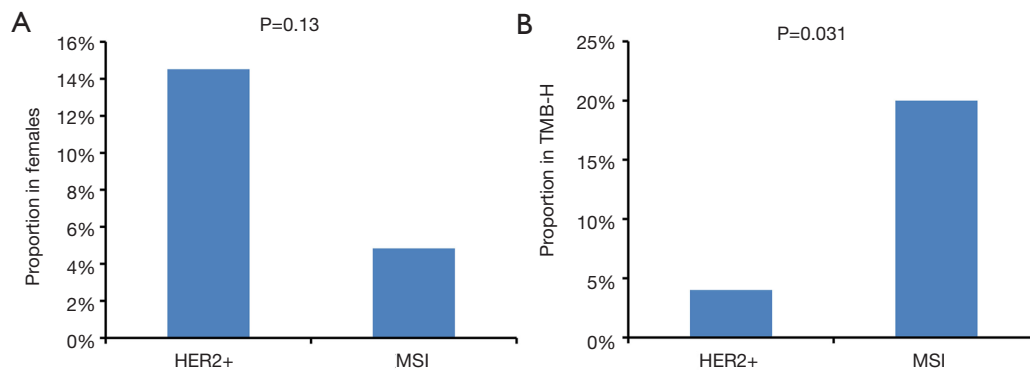


Figure 5 Negative correlation between *HER2* amplification and MSI status. (A) The different proportions of *HER2*+ and MSI in female patients; (B) the significantly different proportions of *HER2*+ and MSI in patients with TMB-H. *HER2*, human epidermal growth factor receptor 2; MSI, microsatellite instability; TMB-H, high tumor mutational burden.

also reported that the most commonly mutated genes in a cohort of patients from Hong Kong were *TP53*, *ARIK1A*, *CDH1*, *APC*, ras homolog gene family member A (*RHOA*), *PIK3CA*, *SMAD4*, *MYC*, and *KRAS* (40). This current study also identified a high frequency of *TP53*, *ARID1A*, *ERBB2*, and *CDH1* gene mutations in 192 Chinese GC patients. In addition, high frequencies of *LRP1B*, *FAT4*, and *CCNE1* mutations were detected, and these have been shown to be important in GC (41-43). To our knowledge, this is the first study to report *LRP1B*, *FAT4*, and *CCNE1* as some of the most frequently mutated genes in GC. These differences suggested that the distribution of GC GAs may be varied based on region.

HER2 mutations can be used for determining the prognosis of GC patients. In a study of Korean GC patients, it was found that in *HER2*-positive patients, loss of *PTEN* expression, and a low *HER2* mean amplification index correlated with resistance to trastuzumab-based therapy and extremely poor prognosis (19). Another study found that Lauren classification combined with *HER2* status was a good prognostic factor for Chinese GC patients. *HER2* negative patients with intestinal type Lauren classification demonstrated the best survival, while patients who were *HER2* positive with diffuse type Lauren classification showed poor survival (44). In this study, the frequency of mutated *HER2* was 14.58%, including 9.38% *HER2* amplification, suggesting that there may be a high proportion of patients with poor prognosis in the Chinese population.

For GC patients with *HER2* mutations, there have been many studies investigating drug therapy. In a single-arm phase II study evaluating the efficacy of combining lapatinib

with capecitabine and oxaliplatin as first line neoadjuvant therapy in untreated *HER2*-overexpressing advanced GC patients, it was found that patients with a high level of *HER2* amplification were more likely to respond to therapy compared to those with a low level of amplification (45). Yoshioka *et al.* demonstrated that *HER2*-amplified cell lines were highly sensitive to the pan-HER inhibitors afatinib and neratinib (46). In a subpopulation analysis of the JACOB trial (NCT01774786), Chinese patients with *HER2*-positive metastatic GC or gastroesophageal junction cancer showed numerically improved overall survival, progression-free survival, overall objective response rate, and a similar safety profile when pertuzumab was added to the treatment regimen of trastuzumab and chemotherapy compared to patients receiving trastuzumab and chemotherapy alone (47). All these studies suggested that *HER2* can be used as a biomarker for adjuvant therapy to improve patient prognosis.

Wang *et al.* performed a meta-analysis of the clinicopathological factors associated with *HER2*-positive GC and found that *HER2*-positive expression was associated with males, intestinal type GC, and well to moderate differentiation (48). This differs from our study in which *HER2* amplification was detected more often in females than in males.

MSI is one of the key factors in GC. Contrary to *HER2* amplification, studies have shown that MSI is associated with good prognosis. Kohlruss *et al.* investigated the role of Epstein-Barr virus (EBV) infections, MSI-H, and MSI-L in 760 GC patients in the context of platinum/5-fluorouracil based preoperative chemotherapy (49). Patients with EBV positive tumors showed the best overall

survival, followed by patients who were MSI-H. MSI-L tumors were significantly associated with poor overall survival (50). Cristescu and colleagues found that MSI tumors were hyper-mutated intestinal-subtype tumors occurring in the antrum, and resulted in a better overall prognosis compared to the mesenchymal-like type tumors (51). Liu *et al.* found that 58.3% of their GC cohort were positive for MSI and concluded that the accumulation of MSI in dysplasia and intestinal metaplasia of gastric mucosa may be an early molecular event during gastric carcinogenesis (52). In this study, MSI was detected in 6.77% of GC patients. This result was consistent with previous reports (35,36), suggesting that MSI can also be used as a biomarker for early detection and prognosis GC patients.

A previous study showed that MSI was significantly associated with females, older patients (mean age of 75 years), distal location, and distal non-diffuse modified Lauren classification in GC. In a survival analysis of patients with stage I–III GC, MSI patients showed a significantly lower risk of cancer-related death (53). However, in the current study, there was no statistical correlation between MSI and gender or age.

Studies on the relationship between *HER2* amplification and MSI are limited. In a molecular profiling study of metastatic colorectal tumors using NGS technology, 5.1% of the patients had *HER2* amplifications. Most of these tumors were microsatellite stable (MSS), with *HER2* copy numbers ranging from 9–190 (54). A retrospective study by Moy *et al.* showed that there was no significant difference in the mean overall survival in patients with and without MSI. In addition, all tumors with MSI were *HER2* negative (55). This was similar to the results in our study where all 13 MSI samples were *HER2* negative.

TMB is an emerging biomarker for predicting immunotherapy responses (29,56). Tumors with TMB-H often have more neoantigens which are beneficial for immunotherapy. TMB-H has been reported to be associated with better outcomes in many cancers (57). A study by Cai and colleagues found that TMB was significantly associated with *HER2* immunohistochemistry status. Higher median TMB values were seen in *HER2* positive tumors, but all TMB-H tumors were *HER2* negative (58). This was in agreement with our study showing that the frequency of *HER2* amplification was lower in TMB-H compared to TMB-L tumors. In addition, this study demonstrated a significant correlation between TMB-H and MSI. Taken together, all these studies suggest that *HER2* amplification

is negatively correlated with microsatellite status in Chinese GC patients, and MSI and *HER2* amplification may be effective biomarkers for predicting prognosis in GC patients.

Conclusions

This study analyzed the genomic features and identified the *HER2* amplification and MSI status in Chinese GC patients. The results revealed that the age of patients was not associated with *HER2* amplification or MSI status. A high frequency of *HER2* amplification was found in female patients and primary lesions, while MSI was detected more frequently in male patients and metastatic foci. MSI status was significantly associated with TMB-H, while *HER2* amplification was not correlated with TMB-H. From this data, we concluded that *HER2* amplification is negatively correlated with the MSI status in Chinese GC patients.

Acknowledgments

We thank OriginMed (Shanghai) Co. Ltd for its contribution to the data analysis of this manuscript.

Funding: None.

Footnote

Reporting Checklist: The authors have completed the MDAR reporting checklist. Available at <http://dx.doi.org/10.21037/jgo-21-47>

Data Sharing Statement: Available at <http://dx.doi.org/10.21037/jgo-21-47>

Conflicts of Interest: All authors have completed the ICMJE uniform disclosure form (available at <http://dx.doi.org/10.21037/jgo-21-47>). The authors have no conflicts of interest to declare.

Ethical Statement: The authors are accountable for all aspects of the work in ensuring that questions related to the accuracy or integrity of any part of the work are appropriately investigated and resolved. All procedures performed in this study involving human participants were in accordance with the Declaration of Helsinki (as revised in 2013). The study was approved by institutional ethics committee of The First Hospital of Shanxi Medical University (No.: 2020-K008) and informed consent was

taken from all the patients.

Open Access Statement: This is an Open Access article distributed in accordance with the Creative Commons Attribution-NonCommercial-NoDerivs 4.0 International License (CC BY-NC-ND 4.0), which permits the non-commercial replication and distribution of the article with the strict proviso that no changes or edits are made and the original work is properly cited (including links to both the formal publication through the relevant DOI and the license). See: <https://creativecommons.org/licenses/by-nc-nd/4.0/>.

References

1. Ferlay J, Soerjomataram I, Dikshit R, et al. Cancer incidence and mortality worldwide: sources, methods and major patterns in GLOBOCAN 2012. *Int J Cancer* 2015;136:E359-86.
2. Cunningham D, Allum WH, Stenning SP, et al. Perioperative chemotherapy versus surgery alone for resectable gastroesophageal cancer. *N Engl J Med* 2006;355:11-20.
3. Macdonald JS, Smalley SR, Benedetti J, et al. Chemoradiotherapy after surgery compared with surgery alone for adenocarcinoma of the stomach or gastroesophageal junction. *N Engl J Med* 2001;345:725-30.
4. Nadauld LD, Ford JM. Molecular profiling of gastric cancer: toward personalized cancer medicine. *J Clin Oncol* 2013;31:838-9.
5. Cancer Genome Atlas Research Network. Comprehensive molecular characterization of gastric adenocarcinoma. *Nature* 2014;513:202-9.
6. Lee SY, Oh SC. Changing strategies for target therapy in gastric cancer. *World J Gastroenterol* 2016;22:1179-89.
7. Chen LT, Oh DY, Ryu MH, et al. Anti-angiogenic Therapy in Patients with Advanced Gastric and Gastroesophageal Junction Cancer: A Systematic Review. *Cancer Res Treat* 2017;49:851-68.
8. Hudziak RM, Lewis GD, Winget M, et al. p185HER2 monoclonal antibody has antiproliferative effects in vitro and sensitizes human breast tumor cells to tumor necrosis factor. *Mol Cell Biol* 1989;9:1165-72.
9. Slamon DJ, Godolphin W, Jones LA, et al. Studies of the HER-2/neu proto-oncogene in human breast and ovarian cancer. *Science* 1989;244:707-12.
10. Verma S, Miles D, Gianni L, et al. Trastuzumab emtansine for HER2-positive advanced breast cancer. *N Engl J Med* 2012;367:1783-91.
11. Hyman DM, Piha-Paul SA, Won H, et al. HER kinase inhibition in patients with HER2- and HER3-mutant cancers. *Nature* 2018;554:189-94.
12. Xi Y, Xu C, Liu Y, et al. The age variation of HER2 immunohistochemistry positive rate in biopsy specimens of gastric cancer. *Pathol Res Pract* 2020;216:152882.
13. Chu Y, Li H, Wu D, et al. HER2 protein expression correlates with Lauren classification and P53 in gastric cancer patients. 2020. DOI: <https://doi.org/10.21203/rs.3.rs-45602/v1>.
14. Shitara K, Yatabe Y, Matsuo K, et al. Prognosis of patients with advanced gastric cancer by HER2 status and trastuzumab treatment. *Gastric Cancer* 2013;16:261-7.
15. Minner S, Jessen B, Stiedenroth L, et al. Low level HER2 overexpression is associated with rapid tumor cell proliferation and poor prognosis in prostate cancer. *Clin Cancer Res* 2010;16:1553-60.
16. Jørgensen JT, Hersom M. HER2 as a Prognostic Marker in Gastric Cancer - A Systematic Analysis of Data from the Literature. *J Cancer* 2012;3:137-44.
17. Dang HZ, Yu Y, Jiao SC. Prognosis of HER2 over-expressing gastric cancer patients with liver metastasis. *World J Gastroenterol* 2012;18:2402-7.
18. Janjigian YY, Werner D, Pauligk C, et al. Prognosis of metastatic gastric and gastroesophageal junction cancer by HER2 status: a European and USA International collaborative analysis. *Ann Oncol* 2012;23:2656-62.
19. Kim C, Lee CK, Chon HJ, et al. PTEN loss and level of HER2 amplification is associated with trastuzumab resistance and prognosis in HER2-positive gastric cancer. *Oncotarget* 2017;8:113494-501.
20. Motoshima S, Yonemoto K, Kamei H, et al. Prognostic implications of HER2 heterogeneity in gastric cancer. *Oncotarget* 2018;9:9262-72.
21. Yamamoto H, Adachi Y, Taniguchi H, et al. Interrelationship between microsatellite instability and microRNA in gastrointestinal cancer. *World J Gastroenterol* 2012;18:2745-55.
22. Nakaji Y, Oki E, Nakanishi R, et al. Prognostic value of BRAF V600E mutation and microsatellite instability in Japanese patients with sporadic colorectal cancer. *J Cancer Res Clin Oncol* 2017;143:151-60.
23. Yamamoto H, Imai K. Microsatellite instability: an update. *Arch Toxicol* 2015;89:899-921.
24. Smyth EC, Wotherspoon A, Peckitt C, et al. Mismatch Repair Deficiency, Microsatellite Instability, and Survival: An Exploratory Analysis of the Medical Research Council Adjuvant Gastric Infusional Chemotherapy (MAGIC)

- Trial. *JAMA Oncol* 2017;3:1197-203.
25. Kim H, An JY, Noh SH, et al. High microsatellite instability predicts good prognosis in intestinal-type gastric cancers. *J Gastroenterol Hepatol* 2011;26:585-92.
 26. Hsu A, Chudasama R, Almhanna K, et al. Targeted therapies for gastroesophageal cancers. *Ann Transl Med* 2020;8:1104.
 27. Patel TH, Cecchini M. Targeted Therapies in Advanced Gastric Cancer. *Curr Treat Options Oncol* 2020;21:70.
 28. Cao J, Chen L, Li H, et al. An Accurate and Comprehensive Clinical Sequencing Assay for Cancer Targeted and Immunotherapies. *Oncologist* 2019;24:e1294-e1302.
 29. Chalmers ZR, Connelly CF, Fabrizio D, et al. Analysis of 100,000 human cancer genomes reveals the landscape of tumor mutational burden. *Genome Med* 2017;9:34.
 30. Kautto EA, Bonneville R, Miya J, et al. Performance evaluation for rapid detection of pan-cancer microsatellite instability with MANTIS. *Oncotarget* 2017;8:7452-63.
 31. Yang P, Javle M, Pang F, et al. Somatic genetic aberrations in gallbladder cancer: comparison between Chinese and US patients. *Hepatobiliary Surg Nutr* 2019;8:604-14.
 32. Hu J, Wang Y, Zhang Y, et al. Comprehensive genomic profiling of small cell lung cancer in Chinese patients and the implications for therapeutic potential. *Cancer Med* 2019;8:4338-47.
 33. Yan B, Yau EX, Bte Omar SS, et al. A study of HER2 gene amplification and protein expression in gastric cancer. *J Clin Pathol* 2010;63:839-42.
 34. Tanner M, Hollmen M, Junttila TT, et al. Amplification of HER-2 in gastric carcinoma: association with Topoisomerase IIalpha gene amplification, intestinal type, poor prognosis and sensitivity to trastuzumab. *Ann Oncol* 2005;16:273-8.
 35. De Craene B, Feng Z, Rondelez E, et al. 697PDetection of microsatellite instability (MSI) with a novel panel of biomarkers in gastric cancer samples. *Ann Oncol* 2017;28.
 36. Polom K, Marano L, Marrelli D, et al. Meta-analysis of microsatellite instability in relation to clinicopathological characteristics and overall survival in gastric cancer. *Br J Surg* 2018;105:159-67.
 37. Chen K, Yang D, Li X, et al. Mutational landscape of gastric adenocarcinoma in Chinese: implications for prognosis and therapy. *Proc Natl Acad Sci U S A* 2015;112:1107-12.
 38. Park J, Yoo HM, Jang W, et al. Distribution of somatic mutations of cancer-related genes according to microsatellite instability status in Korean gastric cancer. *Medicine* 2017;96:e7224.
 39. Jia F, Teer JK, Knepper TC, et al. Discordance of Somatic Mutations Between Asian and Caucasian Patient Populations with Gastric Cancer. *Mol Diagn Ther* 2017;21:179-85.
 40. Wang K, Yuen ST, Xu J, et al. Whole-genome sequencing and comprehensive molecular profiling identify new driver mutations in gastric cancer. *Nat Genet* 2014;46:573-82.
 41. Cai J, Feng D, Hu L, et al. FAT4 functions as a tumour suppressor in gastric cancer by modulating Wnt/beta-catenin signalling. *Br J Cancer* 2015;113:1720-9.
 42. Takeda H, Rust AG, Ward JM, et al. Sleeping Beauty transposon mutagenesis identifies genes that cooperate with mutant Smad4 in gastric cancer development. *Proc Natl Acad Sci U S A* 2016;113:E2057-65.
 43. Ooi A, Oyama T, Nakamura R, et al. Gene amplification of CCNE1, CCND1, and CDK6 in gastric cancers detected by multiplex ligation-dependent probe amplification and fluorescence in situ hybridization. *Hum Pathol* 2017;61:58-67.
 44. Qiu M, Zhou Y, Zhang X, et al. Lauren classification combined with HER2 status is a better prognostic factor in Chinese gastric cancer patients. *BMC Cancer* 2014;14:823.
 45. Kim ST, Banks KC, Pectasides E, et al. Impact of genomic alterations on lapatinib treatment outcome and cell-free genomic landscape during HER2 therapy in HER2+ gastric cancer patients. *Ann Oncol* 2018;29:1037-48.
 46. Yoshioka T, Shien K, Namba K, et al. Antitumor activity of pan-HER inhibitors in HER2-positive gastric cancer. *Cancer Sci* 2018;109:1166-76.
 47. Liu T, Qin Y, Li J, et al. Pertuzumab in combination with trastuzumab and chemotherapy for Chinese patients with HER2-positive metastatic gastric or gastroesophageal junction cancer: a subpopulation analysis of the JACOB trial. *Cancer Commun (Lond)* 2019;39:38.
 48. Wang HB, Liao XF, Zhang J. Clinicopathological factors associated with HER2-positive gastric cancer: A meta-analysis. *Medicine* 2017;96:e8437.
 49. Kohlruss M, Grosser B, Krenauer M, et al. Prognostic implication of molecular subtypes and response to neoadjuvant chemotherapy in 760 gastric carcinomas: role of Epstein-Barr virus infection and high- and low-microsatellite instability. *J Pathol Clin Res*, 2019, 5: 227-239.
 50. Borderud SP, Li YL, Burkhalter JE, et al. Electronic cigarette use among patients with cancer: characteristics of electronic cigarette users and their smoking cessation outcomes. *Cancer*, 2014, 120: 3527-35. .
 51. Cristescu R, Lee J, Nebozhyn M, et al. Molecular analysis

- of gastric cancer identifies subtypes associated with distinct clinical outcomes. *Nat Med* 2015;21:449-56.
52. Liu P, Zhang XY, Shao Y, et al. Microsatellite instability in gastric cancer and pre-cancerous lesions. *World J Gastroenterol* 2005;11:4904-7.
53. Martinez-Ciarpaglini C, Fleitas-Kanonnikoff T, Gambardella V, et al. Assessing molecular subtypes of gastric cancer: microsatellite unstable and Epstein-Barr virus subtypes. Methods for detection and clinical and pathological implications. *ESMO Open* 2019;4:e000470.
54. Gong J, Cho M, Sy M, et al. Molecular profiling of metastatic colorectal tumors using next-generation sequencing: a single-institution experience. *Oncotarget* 2017;8:42198-213.
55. Moy AP, Shahid M, Ferrone CR, et al. Microsatellite instability in gallbladder carcinoma. *Virchows Archiv* 2015;466:393-402.
56. Vanderwalde A, Spetzler D, Xiao N, et al. Microsatellite instability status determined by next-generation sequencing and compared with PD-L1 and tumor mutational burden in 11,348 patients. *Cancer Med* 2018;7:746-56.
57. Maleki Vareki S. High and low mutational burden tumors versus immunologically hot and cold tumors and response to immune checkpoint inhibitors. *J Immunother Cancer* 2018;6:157.
58. Cai H, Jing C, Chang X, et al. Mutational landscape of gastric cancer and clinical application of genomic profiling based on target next-generation sequencing. *J Transl Med* 2019;17:189.
- (English Language Editor: J. Teoh)

Cite this article as: Huang H, Wang Z, Li Y, Zhao Q, Niu Z. Amplification of the human epidermal growth factor receptor 2 (*HER2*) gene is associated with a microsatellite stable status in Chinese gastric cancer patients. *J Gastrointest Oncol* 2021;12(2):377-387. doi: 10.21037/jgo-21-47

Appendix 1

The gene list of YuanSuTM450 gene panel

ABL1 ABL2 ACVR1B ACVR2A ADAM29 ADGRA2 AKT1 AKT2 AKT3 ALK
 AMER1 APC APEX1 AR ARAF ARFRP1 ARID1AARID1BARID2 ASXL1 ATF1 ATM ATR
 ATRX AURKA AURKB AXIN1 AXIN2 AXL BAP1 BARD1 BCL2 BCL2L1 BCL2L11 BCL2L2
 BCL6 BCOR BCORL1 BCR BIRC5 BLK BLM BMPR1A BMX BRAF BRCA1 BRCA2
 BRD4 BRIP1 BTG1 BTK CAMTA1 CARD11 CBF1 CBL CCND1CCND2CCND3CCNE1
 CD274 CD79A CD79B CDC73 CDH1 CDK12 CDK4 CDK6 CDK8 CDKN1A CDKN1B
 CDKN2A CDKN2B CDKN2C CEBPA CFTR CHD2 CHD4 CHEK1 CHEK2 CIC
 COL1A1 CRBN CREB3L1 CREB3L2 CREBBP CRKL CRLF2 CSF1 CSF1R CSK
 CSNK1A1 CTCF CTNNA1 CTNNA1 CTNNA1 CUL3 CXCR4 CYLD CYP17A1 CYP2D6
 DAXX DDR1 DDR2 DICER1 DNMT3A DOT1LDPYD EGF EGFR EMSY EP300 EPCAM
 EPHA2 EPHA3 EPHA5 EPHA7 EPHB1 ERBB2 ERBB3 ERBB4 ERCC1 ERG ERFF1 ESR1 ETV1 ETV4
 ETV5 ETV6 EWSR1 EZH2 FAM135B TENT5C FANCA FANCC FANCD2 FANCE FANCF
 FANCG FANCL FANCM FAS FAT1 FAT3 FAT4 FBXW7 FEN1 FEV FGF10 FGF12 FGF14
 FGF19 FGF23 FGF3 FGF4 FGF6 FGF7 FGFR1 FGFR2 FGFR3 FGFR4 FGR FH FLCN FLI1
 FLT1 FLT3 FLT4 FOS FOXL2 FOXO1 FOXP1 FRS2 FUBP1 FUS FYN GABRA6
 GATA1 GATA2 GATA3 GATA4 GATA6 GID4 GLI1 GLI2 GLI3 GNA11 GNA13 GNAQ GNAS
 GRIN2A GRM3 GSK3B H3-3A HCK HDAC9HGF HNF1A HRAS HSD3B1 HSP90AA1
 HTATIP2 IDH1 IDH2 IGF1R IGF2 IKBKE IKZF1 IL7R INHBA INPP4BIRF2 IRF4
 IRS2 ITK JAK1 JAK2 JAK3 JUN KAT6A KDM5AKDM5BKDM5C KDM6AKDR KEAP1
 KEL KIT KLHL6 KMT2AKMT2CKMT2D KRAS LCK LIMK1 LMO1 LRP1 LRP1B LRP2
 LYN LZTR1 MACC1MAGI2 MAP2K1 MAP2K2 MAP2K4 MAP3K1 MAP3K13
 MAP4K5 MCL1 MDM2 MDM4 MED12 MEF2B MEN1 MERTK MET MGMT MITF MLH1
 MPL MRE11 MS4A1 MSH2 MSH6 MST1R MTOR MUTYH MYB MYC MYCL MYCN MYD88
 NBN NCOA2NCOR1NEK11 NF1 NF2 NFE2L2 NFIB NFKBIA NKX2-1NOTCH1
 NOTCH2 NOTCH3 NOTCH4 NPM1 NR4A3 NRAS NRG1 NRG3 NSD1 NTRK1
 NTRK2 NTRK3 NUP93 PAK3 PALB2 PRKN PARP1 PARP2 PARP3 PARP4 PAX5 PBRM1 PCA3 PDCD1
 PDCD1LG2 PDGFB PDGFRA PDGFRB PDK1 PIK3C2B PIK3CAPIK3CBPIK3CD
 PIK3CG PIK3R1 PIK3R2 PKD2 PLA2G1B PLCG2 PMS2 POLB POLD1 POLE PPP2R1A
 PRDM1 PREX2 PRKACA PRKAR1A PRKCI PRKDCPRSS1 PRSS8 PTCH1 PTEN PTK2 PTK6
 PTPN11 QKI RAC1 RAD50 RAD51 RAD51B RAD51C RAD51D RAD52
 RAD54B RAD54L RAF1 RANBP2 RARA RB1 RBM10 RECQLREL RELB RELB
 RET RHBDF2 RHOA RICTOR RNF43 ROCK1 ROCK2 ROS1 RPTORRUNX1 RUNX1T1
 RXRA SDHA SDHB SDHC SDHD SETD2 SF3B1 SIK1 SLIT2 SMAD2 SMAD3 SMAD4 SMARCA4
 SMARCB1 SMARCD1 SMO SNCAIP SOCS1 SOX10 SOX2 SOX9 SPEN SPINK1SPOP
 SPTA1 SRC SRMS SS18 SSX1 STAG2 STAT3 STAT4 STK11 STK24 SUFU SYK TAF1 TBX3
 TCF7L2 TEK TERT TET1 TET2 TET3 TFE3 TGFBR1 TGFBR2 TIE1 TIPARP
 TMPRSS2 TNFAIP3 TNFRSF14 TNFSF11 TNFSF13B TNK2 TOP1 TOP2A TP53
 TPMT TSC1 TSC2 TSHR TYK2 U2AF1 UGT1A1 VEGFA VHL WEE1 WEE2 NSD2 CCN6
 WT1 XIAP XPO1 XRCC2 XRCC3 YES1 ZBTB2 ZNF217ZNF703ZNF750

Table S1 Altered genes in 192 Chinese gastric cancer patients

	CNV	Fusion	Long Indel	SNV/Short Indel	Total	Ratio
TP53	0	1	1	129	131	68.23%
ARID1A	0	0	1	35	36	18.75%
LRP1B	0	0	2	31	33	17.19%
ERBB2	18	0	0	10	28	14.58%
FAT4	0	0	2	24	26	13.54%
CDH1	3	1	1	19	24	12.50%
CCNE1	20	0	0	1	21	10.94%
PIK3CA	0	0	0	19	19	9.90%
KMT2D	0	0	1	17	18	9.38%
ERBB3	2	0	0	15	17	8.85%
APC	0	0	0	17	17	8.85%
RNF43	0	0	2	15	17	8.85%
ATM	1	1	0	14	16	8.33%
SMAD4	0	0	0	16	16	8.33%
ACVR2A	0	0	0	15	15	7.81%
KMT2C	0	0	1	14	15	7.81%
CDK12	9	0	0	5	14	7.29%
KRAS	8	0	0	6	14	7.29%
ARID2	2	0	1	11	14	7.29%
TGFBR2	0	0	0	14	14	7.29%
CDKN2A	4	0	1	8	13	6.77%
SPTA1	1	0	0	12	13	6.77%
LRP1	0	1	3	9	13	6.77%
FGFR2	12	0	0	0	12	6.25%
FBXW7	0	0	0	12	12	6.25%
GLI3	0	0	0	12	12	6.25%
CCND1	11	0	0	0	11	5.73%
FGF3	10	0	0	1	11	5.73%
GATA4	10	0	0	1	11	5.73%
RARA	10	0	0	1	11	5.73%
TOP2A	10	0	0	1	11	5.73%
SMARCA4	1	0	2	8	11	5.73%
RHOA	0	0	0	11	11	5.73%
PIK3R1	0	0	1	10	11	5.73%
FGF19	10	0	0	0	10	5.21%
FGF4	10	0	0	0	10	5.21%
BLK	9	0	0	1	10	5.21%
GRM3	2	0	0	8	10	5.21%
VEGFA	9	0	0	0	9	4.69%
EGFR	4	0	0	5	9	4.69%
CTNNB1	1	0	0	8	9	4.69%
GNAS	1	0	0	8	9	4.69%
EPHA5	0	0	0	9	9	4.69%
MYC	8	0	0	0	8	4.17%
BCOR	1	0	1	6	8	4.17%
CIC	1	0	1	6	8	4.17%
PTEN	1	1	1	5	8	4.17%
BRCA1	0	1	0	7	8	4.17%
FAT3	0	0	1	7	8	4.17%
PTCH1	0	0	1	7	8	4.17%
CREBBP	0	1	0	6	8	4.17%
GATA6	6	0	1	1	7	3.65%
TERT	5	0	1	1	7	3.65%
FAM135B	2	0	0	5	7	3.65%
EPHA3	1	0	0	6	7	3.65%
PREX2	1	0	0	6	7	3.65%
IKZF1	0	0	0	7	7	3.65%
LRP2	0	0	0	7	7	3.65%
NTRK3	0	0	0	7	7	3.65%
SPEN	0	0	0	7	7	3.65%
ALK	0	1	0	6	7	3.65%
BRC2	0	2	0	5	7	3.65%
MCL1	6	0	0	0	6	3.13%
STK11	4	0	0	2	6	3.13%
MET	2	1	0	3	6	3.13%
NTRK1	2	1	0	3	6	3.13%
AXIN1	1	0	0	5	6	3.13%
NF1	1	0	0	5	6	3.13%
NOTCH3	1	0	0	5	6	3.13%
NOTCH4	1	0	0	5	6	3.13%
CFTR	1	2	0	3	6	3.13%
BRAF	0	0	0	6	6	3.13%
CARD11	0	0	0	6	6	3.13%
EPHB1	0	0	0	6	6	3.13%
ERBB4	0	0	0	6	6	3.13%
FAT1	0	0	0	6	6	3.13%
PBRM1	0	0	0	6	6	3.13%
RAD50	0	0	0	6	6	3.13%
RUNX1T1	0	0	0	6	6	3.13%
SLIT2	0	0	0	6	6	3.13%
TET2	0	0	0	6	6	3.13%
TGFBR1	0	0	0	6	6	3.13%
TSC2	0	0	0	6	6	3.13%
ARID1B	0	0	1	5	6	3.13%
RUNX1	0	0	1	5	6	3.13%
SETD2	0	1	1	4	6	3.13%
CCND3	5	0	0	0	5	2.60%
CDKN2B	4	0	0	1	5	2.60%
ZNF217	4	0	0	1	5	2.60%
DDR2	2	0	0	3	5	2.60%
PTK2	2	0	0	3	5	2.60%
CUL3	1	0	0	4	5	2.60%
FANCM	1	0	0	4	5	2.60%
MAP3K13	1	0	0	4	5	2.60%
NOTCH2	1	0	0	4	5	2.60%
CASP8	0	0	0	5	5	2.60%
INHBA	0	0	0	5	5	2.60%
NOTCH1	0	0	0	5	5	2.60%
PIK3CG	0	0	0	5	5	2.60%
PRKDC	0	0	0	5	5	2.60%
ROS1	0	0	0	5	5	2.60%
TAF1	0	0	0	5	5	2.60%
RANBP2	0	1	0	4	5	2.60%
MLH1	0	0	1	4	5	2.60%
EMSY	4	0	0	0	4	2.08%
DDR1	3	0	0	1	4	2.08%
FLT1	3	0	0	1	4	2.08%
MDM2	3	0	0	1	4	2.08%
WT1	2	0	0	2	4	2.08%
ASXL1	1	0	0	3	4	2.08%
CBL	1	0	0	3	4	2.08%
MAP2K4	1	0	1	2	4	2.08%
ACVR1B	0	0	0	4	4	2.08%
AMER1	0	0	0	4	4	2.08%
ATR	0	0	0	4	4	2.08%
ATRX	0	0	0	4	4	2.08%
AXIN2	0	0	0	4	4	2.08%
CSF1R	0	0	0	4	4	2.08%
EP300	0	0	0	4	4	2.08%
EPHA7	0	0	0	4	4	2.08%
FOXO1	0	0	0	4	4	2.08%
GABRA6	0	0	0	4	4	2.08%
GRIN2A	0	0	0	4	4	2.08%
HDAC9	0	0	0	4	4	2.08%
KMT2A	0	0	0	4	4	2.08%
MAGI2	0	0	0	4	4	2.08%
MAP3K1	0	0	0	4	4	2.08%
MED12	0	0	0	4	4	2.08%
MRE11	0	0	0	4	4	2.08%
MSH6	0	0	0	4	4	2.08%
MTOR	0	0	0	4	4	2.08%
NRG3	0	0	0	4	4	2.08%
PTPN11	0	0	0	4	4	2.08%
SMAD2	0	0	0	4	4	2.08%
SNCAIP	0	0	0	4	4	2.08%
CAMTA1	0	1	0	3	4	2.08%
CHD4	0	1	0	3	4	2.08%
B2M	0	0	1	3	4	2.08%
STAG2	0	0	1	3	4	2.08%
POLE	0	2	0	2	4	2.08%
CDC73	0	1	1	2	4	2.08%
FLT3	3	0	0	0	3	1.56%
FOS	3	0	0	0	3	1.56%
FRS2	3	0	0	0	3	1.56%
TNFSF13B	3	0	0	0	3	1.56%
FAS	2	0	0	1	3	1.56%
IL7R	2	0	0	1	3	1.56%
JAK3	2	0	0	1	3	1.56%
PIK3R2	2	0	0	1	3	1.56%
RICTOR	2	0	0	1	3	1.56%
ARFRP1	1	0	0	2	3	1.56%
BCL6	1	0	0	2	3	1.56%
BMPR1A	1	0	0	2	3	1.56%
FGF10	1	0	0	2	3	1.56%
FOXP1	1	0	0	2	3	1.56%
GATA3	1	0	0	2	3	1.56%
IRS2	1	0	0	2	3	1.56%
KDM6A	1	0	0	2	3	1.56%
MITF	1	0	0	2	3	1.56%
RET	1	0	0	2	3	1.56%
STAT3	1	0	0	2	3	1.56%
TNK2	1	1	0	1	3	1.56%
KLHL6	1	0	1	1	3	1.56%
FANCA	1	2	0	0	3	1.56%
CREB3L1	1	0	2	0	3	1.56%
AR	0	0	0	3	3	1.56%
BAP1	0	0	0	3	3	1.56%
CDKN1B	0	0	0	3	3	1.56%
CTCF	0	0	0	3	3	1.56%
DNMT3A	0	0	0	3	3	1.56%
ERG	0	0	0	3	3	1.56%
FANCD2	0	0	0	3	3	1.56%
FGF23	0	0	0	3	3	1.56%
GLI1	0	0	0	3	3	1.56%
GLI2	0	0	0	3	3	1.56%
HNF1A	0	0	0	3	3	1.56%
JAK1	0	0	0	3	3	1.56%
KDR	0	0	0	3	3	1.56%
MAP2K1	0	0	0	3	3	1.56%
NBN	0	0	0	3	3	1.56%
PAK3	0	0	0	3	3	1.56%
PDGFRA	0	0	0	3	3	1.56%
POLD1	0	0	0	3	3	1.56%
PRSS1	0	0	0	3	3	1.56%
RBM10	0	0	0	3	3	1.56%
SMAD3	0	0	0	3	3	1.56%
SOX9	0	0	0	3	3	1.56%
TYK2	0	0	0	3	3	1.56%
XRCC2	0	0	0	3	3	1.56%
CHD2	0	1	0	2	3	1.56%
FANCG	0	1	0	2	3	1.56%
NTRK2	0	1	0	2	3	1.56%
BLM	0	0	1	2	3	1.56%
PARP4	0	0	1	2	3	1.56%
RECQL	0	0	1	2	3	1.56%
ETV6	0	2	0	1	3	1.56%
PALB2	0	1	1	1	3	1.56%
APEX1	2	0	0	0	2	1.04%
CDK6	2	0	0	0	2	1.04%
MEF2B	2	0	0	0	2	1.04%
BRD4	1	0	0	1	2	1.04%
FGF14	1	0	0	1	2	1.04%
HCK	1	0	0	1	2	1.04%
LIMK1	1	0	0	1	2	1.04%
LMO1	1	0	0	1	2	1.04%
MYCN	1	0	0	1	2	1.04%
PPP2R1A	1	0	0	1	2	1.04%
PRKCI	1	0	0	1	2	1.04%
RAD52	1	0	0	1	2	1.04%
ROCK2	1	0	0	1	2	1.04%
SOX2	1	0	0	1	2	1.04%
SRMS	1	0	0	1	2	1.04%
STAT4	1	0	0	1	2	1.04%
TBX3	1	0	0	1	2	1.04%
TOP1	1	0	0	1	2	1.04%
MYB	1	1	0	0	2	1.04%
AKT1	0	0	0	2	2	1.04%
BCL2	0	0	0	2	2	1.04%
BCORL1	0	0	0	2	2	1.04%
BRIP1	0	0	0	2	2	1.04%
CTNNA1	0	0	0	2	2	1.04%
CXCR4	0	0	0	2	2	1.04%
DOT1L	0	0	0	2	2	1.04%
EGF	0	0	0	2	2	1.04%
EPCAM	0	0	0	2	2	1.04%
ERRF1	0	0	0	2	2	1.04%
ESR1	0	0	0	2	2	1.04%
ETV1	0	0	0	2	2	1.04%
FEN1	0	0	0	2	2	1.04%
FGFR3	0	0	0	2	2	1.04%
FGFR4	0	0	0	2	2	1.04%
FOXL2	0	0	0	2	2	1.04%
FYN	0	0	0	2	2	1.04%
HGF	0	0	0	2	2	1.04%
IDH1	0	0	0	2		